

tube axis is directly observed in the STM image of Fig. 2A. The measured period of 16 Å reveals that the second layer of the tube is rotated relative to the first layer by 9°. The first and the second cylindrical layers have chiral angles of 5° and -4°, respectively, showing that the tubes are indeed composed of at least two coaxial graphitic cylinders with different helicities.

In our experiments, hot vapor is suddenly quenched on a cold surface. The substrate is atomically flat and chemically inert. This leads to cooling and supersaturation of the incoming vapor on a nearly noninteracting surface. The resulting quasi-free growth conditions resemble those for vapor-phase fullerene formation. This method gives a new approach to understand the formation of novel hollow graphitic structures. Our observations suggest that the growth to tubular rather than spherical configurations is preferred for "giant fullerenes."

REFERENCES AND NOTES

1. S. Iijima, *Nature* **354**, 56 (1991); _____, T. Ichihashi, Y. Ando, *ibid.* **356**, 776 (1992).
2. S. Iijima, P. M. Ajayan, T. Ichihashi, *Phys. Rev.*

- Let.* **69**, 3100 (1992).
3. T. W. Ebbensen and P. M. Ajayan, *Nature* **358**, 220 (1992).
4. R. Saito, M. Fujita, G. Dresselhaus, M. S. Dresselhaus, *Appl. Phys. Lett.* **60**, 2204 (1992).
5. N. Hamada, S. Samada, A. Oshiyama, *Phys. Rev. Lett.* **68**, 1579 (1992).
6. J. W. Mintmire *et al.*, *ibid.*, p. 631.
7. K. Harigaya, *Phys. Rev. B* **45**, 12017 (1992).
8. M. Peterson and J. Q. Broughton, *Phys. Rev. Lett.* **69**, 2689 (1992).
9. T. Lenosky *et al.*, *Nature* **355**, 333 (1992).
10. D. Vanderbilt and J. Tersoff, *Phys. Rev. Lett.* **68**, 511 (1992).
11. M. O'Keeffe *et al.*, *ibid.*, p. 2325.
12. C. R. Clemmer and T. P. Beebe, Jr., *Science* **251**, 640 (1991).
13. G. Tibbetts, *J. Cryst. Growth* **66**, 632 (1984).
14. M. S. Dresselhaus, G. Dresselhaus, R. Saito, *Phys. Rev. B* **45**, 6234 (1992).
15. M. Kuwabara, D. R. Clarke, D. A. Smith, *Appl. Phys. Lett.* **56**, 2396 (1990).
16. J. Xhie, K. Sattler, M. Ge, N. Venkatasmaran, *Phys. Rev. B*, in press.
17. P. I. Oden *et al.*, *Surf. Sci. Lett.* **254**, L454 (1991).
18. J. W. Lyding *et al.*, *J. Vac. Sci. Technol.* **A6**, 363 (1988).
19. J. E. Buckley *et al.*, *ibid.* **B9**, 1079 (1991).
20. V. Elings and F. Wudl, *ibid.* **A6**, 412 (1988).
21. D. Tomanek *et al.*, *Phys. Rev. B* **35**, 7790 (1987).
22. We thank N. Venkateswaran and J. Xhie for helpful discussions. Financial support from the National Science Foundation, grant DMR-9106374, is gratefully acknowledged.

21 December 1991; accepted 16 February 1993

Oxygen Diffusion in Perovskite: Implications for Electrical Conductivity in the Lower Mantle

Bjarni Gautason and Karlis Muehlenbachs

Experimental determination of oxygen self-diffusion in CaTiO₃ perovskite, a structural analog of (Mg,Fe)SiO₃ perovskite, confirms a theoretical relation between diffusion constants and anion porosity. Oxygen diffusion rates in (Mg,Fe)SiO₃ perovskite calculated with this relation increase by about eight orders of magnitude through the lower mantle. Electrical conductivity values calculated from these diffusion rates are consistent with inferred conductivity values for the lower mantle. This result suggests that the dominant conductivity mechanism in the deep mantle is ionic.

The lower mantle is the Earth's largest silicate and oxygen reservoir, constituting roughly half of the planet's volume. The dominant phase in the lower mantle, (Mg,Fe)SiO₃ perovskite, accounts for >85% of its volume (1). Consequently, diffusion of major elements in this phase may dominate dynamic processes in the lower mantle. Only recently have measurements of the physical properties of (Mg,Fe)SiO₃ perovskite at pressures and temperatures that correspond to those of the lower mantle become possible (2, 3). These measurements are still limited because of sample size and constraints of the experimental apparatus. In the absence of direct experimental determination, diffusion rates at very high

pressure and temperature may be inferred by experimental study of analog phases, empirical modeling, or theoretical calculations. The data from these approaches may provide a framework to discuss subjects such as isotopic equilibration rates, mantle rheology, chemical transfer between mantle and core, and ionic conductivity.

In this report we provide data on oxygen diffusion in CaTiO₃ perovskite, a phase commonly used as an analog to (Mg,Fe)SiO₃ perovskite (4). Both CaTiO₃ and (Mg,Fe)SiO₃ perovskite are orthorhombic ABO₃ compounds, with a similar tolerance factor (5) and, hence, similar thermochemical properties (6). The experimentally determined oxygen diffusion constants for CaTiO₃ are consistent with empirical rules that relate diffusion constants to crystal porosity (7). Therefore, we propose that

the empirical relations may be used to estimate oxygen diffusion constants for (Mg,Fe)SiO₃ perovskite.

Diffusion is a thermally activated process and is commonly described by the Arrhenius relation

$$D = D_0 \exp(-Q/RT) \quad (1)$$

where D is the diffusion coefficient, D_0 is a constant, Q is the activation energy, R is the gas constant, and T is absolute temperature. When this relation holds, a plot of the logarithm of the diffusion coefficients versus the inverse temperatures yields a straight line. To measure oxygen diffusion in CaTiO₃ perovskite, we partially equilibrated aliquots of perovskite powder with CO₂ gas at temperatures between 900° and 1300°C in a 1-atm furnace. Several experiments were done at each temperature, with varied grain size and run time (8). The data from our experiments (Fig. 1) fit an Arrhenius relation with an activation energy (derived from the slope on Fig. 1) of 313 ± 10 kJ mol⁻¹ and a preexponential factor D_0 of $5.0^{+7.8}_{-3.1}$ cm² s⁻¹.

The experimentally derived oxygen diffusion constants Q and D_0 for CaTiO₃ perovskite are consistent with a recent empirical model that relates the activation energy for oxygen diffusion and the preexponential factor ($\ln D_0$) to the anion porosity (Φ) of crystals (7). The anion porosity is a measure of the volume fraction not occupied by anions and is defined as $1 - (V_A/V)$, where V_A is the volume of anions in the unit cell and V is the unit cell volume (9). Data from 1-atm oxygen diffusion experiments on several minerals (Table 1) illustrate a well-defined linear relation (Fig. 2A) between anion porosity and the activation energy. In contrast, the relation between porosity and $\ln D_0$ (Fig. 2B) shows considerable scatter. In both plots, the scatter is significantly reduced if the data from a single laboratory are considered (7), which suggests that some scatter stems from interlaboratory comparison. Furthermore, the activation energy and $\ln D_0$ cannot be determined independently, and small uncertainties in the slope (Q) will lead to large uncertainties in D_0 .

The linear relations may be combined to give an equation that relates anhydrous oxygen diffusion to temperature and anion porosity (7, 10)

$$\ln D = A + B\Phi - [(L + M\Phi)10^3/RT] \quad (2)$$

The constants A and B are the intercept and slope, respectively, in the linear relation between $\ln D_0$ and Φ , and the relation between Q and Φ is similarly described by the constants L and M (Fig. 2, A and B). We obtained $A = 36.5 \pm 7.7$, $B = -1.01 \pm 0.17$, $L = 1116 \pm 60$, and $M = -18.6 \pm 1.3$ from the values in Table 1 (11). The

Department of Geology, University of Alberta, Edmonton T6G 2E3, Canada.

data on CaTiO₃ perovskite are consistent with the trend delineated by the other minerals. The predicted activation energy is within experimental error. The predicted D₀, however, is one-tenth of the experimentally observed value. Nevertheless, the agreement is satisfactory given the large uncertainties inherent in the determination of D₀.

Application of the model to diffusion within the Earth requires that the anion porosity of (Mg,Fe)SiO₃ perovskite as a function of temperature and pressure be determined from its equation of state (EOS). We calculated porosity from an appropriate room temperature EOS (12), which reproduces all available (at T ~ 300 K) pressure-volume (P-V) data on (Mg,Fe)-SiO₃ perovskite. This EOS strictly applies to pure MgSiO₃ perovskite. However, recent studies have shown that the P-V relations for (Mg_{1-x},Fe_x)SiO₃ perovskite are insensitive to compositional variation in the range between X = 0 and X = 0.2 (2). Furthermore, the thermal expansion coefficient α of (Mg,Fe)SiO₃ perovskite decreases rapidly from low pressures up to 30 GPa, where the increase in unit cell volume is <2% (relative) between 300 and 1100 K (13); at higher pressures, the effect is even smaller. Consequently, the thermal expansion of the unit cell of (Mg,Fe)SiO₃ perovskite at lower mantle conditions has minimal effect on the porosity and may be ignored. To calculate the anion porosity, one must also know the compressibility of Si-O and Mg-O polyhedra. However, there are few data available on the compressibility of polyhedra in silicates except in the limited pressure range of 0 to 5 GPa (14). We assumed that the reduction of anion porosity is proportional to the compression of the unit cell, which implies that the reduction of unit cell volume is achieved in part by direct compression of the oxygen anions. The ionic radius of O²⁻ at 0 GPa is taken to be 1.40 Å from consideration of average bond lengths obtained in x-ray diffraction studies on (Mg,Fe)-SiO₃ (15). If we assume that at lower mantle pressures shortening of the bonds is taken up equally by the cations and anions, then the value for the oxygen radius at 135 GPa is 1.27 Å (Fig. 3).

A corollary to the model is that, at a certain temperature, diffusion will be independent of anion porosity and hence of pressure. This temperature, which we refer to as an isokinetic temperature (T_i), can be determined by differentiation of Eq. 2 and solving for (∂lnD/∂Φ)_T = 0.

$$\left(\frac{\partial \ln D}{\partial \Phi}\right)_T = B - \frac{10^3 M}{RT} \quad (3)$$

Substitution of our values for the constants in Eq. 2 yields T_i ≈ 1900°C. At T_i, oxygen

will diffuse at the same rate in all silicates and oxides regardless of their anion porosity. Isokinetic temperature is similar to Hart's (16) crossover temperature T*, at which in a given matrix all species diffuse at the same rate. The calculated T_i is greater than temperatures encountered in the Earth's crust and upper mantle. However, it is well within the range of lower mantle temperatures.

To examine further the effect of pressure and temperature on diffusion as a function of anion porosity we plotted ΔlnD/ΔΦ versus T⁻¹ (Fig. 4). Where ΔlnD refers to lnD₂ - lnD₁ at some arbitrary pressures 1 and 2 and ΔΦ refers to Φ₂ - Φ₁ at those same pressures. The plot yields a line of slope 10³ M/R and intercept B (see Eq. 3). At temperatures < T_i, ΔlnD/ΔΦ is positive and oxygen diffusion rates decrease with decreasing porosity (increasing pressure) at constant temperature. However, at temperatures > T_i this trend is reversed, ΔlnD/ΔΦ

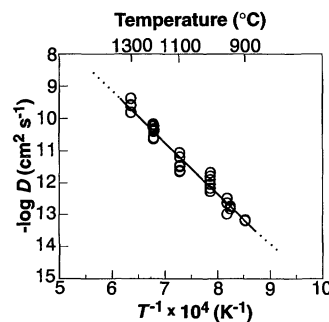


Fig. 1. Oxygen diffusion coefficients for CaTiO₃ perovskite plotted against inverse temperature [(degrees kelvin)⁻¹].

Table 1. Diffusion constants for anhydrous oxygen diffusion in a variety of silicate and oxides. All references are in (26), except leucite (6) and perovskite (this work). Uncertainties are in parentheses.

| Mineral | Φ (%) | ln D ₀ (cm ² s ⁻¹) | Q (kJ mol ⁻¹) |
|---|-------|--|---------------------------|
| CaTiO ₃ perovskite | 43.3 | 1.61 (1) | 313 (10) |
| Leucite | 56.9 | -25.07 (1.4) | 59 (13) |
| Nepheline | 53.1 | -18.95 | 105 (11) |
| Melilite | 51.4 | -11.66 | 140 (0.5) |
| Melilite (Ak ₅₀ Ge ₅₀) | 51.8 | -11.84 | 133 (0.5) |
| Melilite (Ak ₇₅ Ge ₂₅) | 49.6 | -11.51 (0.9) | 236 (8) |
| Anorthite | 42.0 | -3.56 | 415 |
| Forsterite | 42.0 | -12.98 | 293 |
| Diopside | 42.4 | 1.84 | 405 (24) |
| Quartz | 46.5 | -15.03 | 221 |
| SiO ₂ glass | 53.5 | -23.85 | 82 (17) |
| Mg-spinel | 36.0 | -0.12 (4) | 439 (67) |
| Mg-spinel | 36.0 | -4.55 (1.3) | 415 (30) |
| Sapphire | 25.5 | 5.60 | 615 (40) |
| MgO | 43.5 | -8.57 (1.4) | 370 (20) |
| α-Fe ₂ O ₃ | 37.1 | 6.45 (2.4) | 405 (25) |

< 0, and oxygen diffusion rates increase with decreasing porosity at constant temperature. Consequently, below a certain depth (where the T_i isotherm is intersected at ~1100 km) in the lower mantle, oxygen diffusion rates increase because of increasing pressure and temperature.

Calculated oxygen diffusion rates in (Mg,Fe)SiO₃ perovskite along a geothermal gradient of the lower mantle (17) increase by about eight orders of magnitude, from ~10⁻¹⁴ to ~10⁻⁶ cm² s⁻¹ through the lower mantle from ~670 km to ~2890 km (18). Thus, oxygen diffusion rates are up to ten orders of magnitude greater in (Mg,Fe)SiO₃ perovskite in the lower mantle than in major upper mantle constituents such as olivine (at ~1200°C). This difference results from a predicted high D₀ and activation energy and, in particular, the modifying effect of high temperatures on the exponential term in the Arrhenius equation. Thus, the effect of temperature

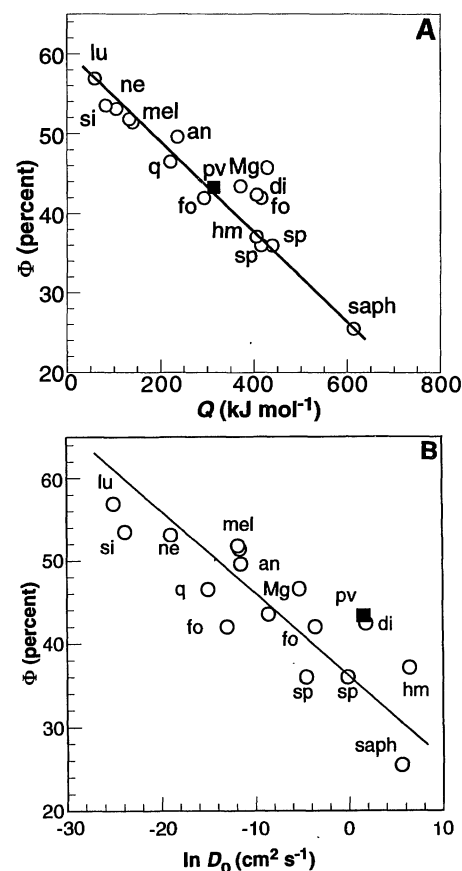


Fig. 2. (A) Relation between activation energy and anion porosity. (B) Relation between the preexponential factor ln D₀ and porosity. Our experimental results for oxygen diffusion in CaTiO₃ perovskite are shown as filled squares. Data and errors on Q and D₀ are given in Table 1. Abbreviations: pv, CaTiO₃ perovskite; lu, leucite; ne, nepheline; mel, melilite; an, anorthite; fo, forsterite; di, diopside; q, quartz; si, SiO₂ glass; sp, Mg-spinel; saph, sapphire; MgO, MgO; hm, α-Fe₂O₃.

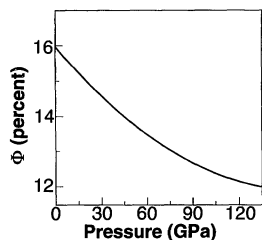


Fig. 3. Calculated anion porosity for MgSiO₃ perovskite plotted against pressure.

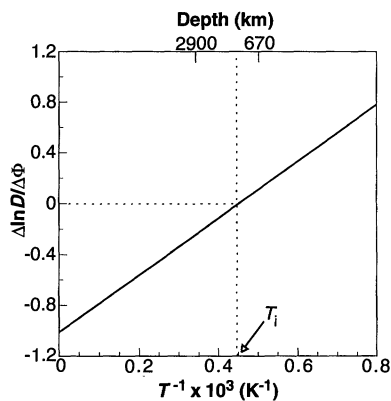


Fig. 4. Plot of $\Delta \ln D / \Delta \Phi$ versus $T^{-1} \times 10^3$. The slope is given by $(\partial Q / \partial \Phi) R^{-1}$, and the intercept is given by $(\partial \ln D_0 / \partial \Phi)$. The isokinetic temperature is indicated, and depth in the mantle, according to Anderson's (17) geothermal gradient, is shown. At temperatures $> T_i$, $\Delta \ln D / \Delta \Phi$ is negative and oxygen diffusion rates increase with increasing pressure at constant temperature. Below T_i , diffusion rates decrease with increasing pressure.

outweighs that of pressure on oxygen diffusion. Our results are supported by theoretical calculations that conclude that (Mg,Fe)-SiO₃ perovskite is a solid electrolyte at high temperatures (~ 4000 and ~ 5000 K) in the lower mantle (20, 21).

Most previous studies have suggested that electronic conduction is the single most important conduction mechanism in the lower mantle (22, 23). However, our work indicates that oxygen diffusion rates in (Mg,-Fe)SiO₃ perovskite are fast enough that ionic conductivity may be an important, and possibly the dominant, conduction mechanism in the lower mantle (20, 22). The total conductivity σ_t of a phase may be written as

$$\sigma_t = \sigma_e + \sigma_i \quad (4)$$

where σ_e and σ_i are the contributions to total conductivity from electronic and ionic conduction, respectively. The contribution from ionic diffusion to the total conductivity may be calculated from the Nernst-Einstein relation (24)

$$\sigma_i / D = N z^2 e^2 / k T \quad (5)$$

where N is the number of ion pairs per cubic centimeter, z and e are the valence

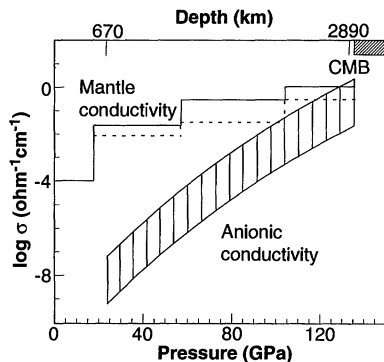


Fig. 5. Comparison of anionic conductivity calculated from oxygen diffusion rates in (Mg,Fe)-SiO₃ perovskite as a function of pressure, and mantle conductivity profiles inferred from secular variations in the Earth's magnetic field. The vertically hatched area is our calculated profile with an assumed error of ± 1 log unit. The solid line is the preferred profile of Ducruix *et al.* (25) and the stippled line marks their lower limit on conductivity. The core mantle boundary (CMB) is indicated.

and charge of the diffusing species (O^{2-}), respectively, and k is Boltzmann's constant. At reasonable lower mantle temperatures, the ionic conduction ($\text{ohm}^{-1} \text{cm}^{-1}$) is $\sim 4 \times 10^4 D$ ($\text{cm}^2 \text{s}^{-1}$).

We have calculated the ionic conductivity in perovskite as a function of depth in the lower mantle. The calculated values are in good agreement with conductivity values inferred from geomagnetic field variations (25), particularly for those close to the base of the lower mantle (Fig. 5). Therefore, we conclude that oxygen transport contributes significantly to the overall electrical conduction in the Earth's lower mantle. These results help explain recent experiments on (Mg,Fe)SiO₃ perovskite and perovskite-bearing assemblages that give apparently contradictory results (23). Although the exact nature of the electrical conductivity of (Mg,Fe)SiO₃ perovskite has not been resolved, our results indicate that the inferred electrical conductivity of the lower mantle does not provide constraints on the composition of the lower mantle.

REFERENCES AND NOTES

- L. G. Liu, *Phys. Earth Planet. Inter.* **11**, 289 (1976); E. Ito and Y. Matsui, *Earth Planet. Sci. Lett.* **38**, 443 (1978); B. O'Neill and R. Jeanloz, *Geophys. Res. Lett.* **17**, 1477 (1990); L. Stixrude, R. J. Hemley, Y. Fei, H. K. Mao, *Science* **257**, 1099 (1992).
- H. K. Mao *et al.*, *J. Geophys. Res.* **96**, 8069 (1991).
- Y. Wang *et al.*, *Science* **251**, 410 (1991).
- S.-I. Karato and P. Li, *ibid.* **255**, 1238 (1992); D. H. Xiong, L. C. Ming, M. H. Manghani, *Phys. Earth Planet. Inter.* **43**, 244 (1986).
- The tolerance factor t is defined as $(r_A + r_O) / 2(r_B + r_O)$, where r denotes the empirical radii of A, B, and O ions.
- A. Navrotsky, in *Structure and Bonding in Crystals*, M. O'Keefe and A. Navrotsky, Eds. (Academic Press, New York, 1981) vol. II, p. 71; in *Perovskite: A Structure of Great Interest to Geophysics and Materials Science*, A. Navrotsky and D. J. Weidner, Eds. (Geophysical Monograph 45, American Geophysical Union, Washington, DC, 1987), p. 67.

- K. Muehlenbachs and C. Connolly, in *Stable Isotope Geochemistry: A Tribute to Samuel Epstein*, H. P. Taylor, Jr., J. R. O'Neill, I. R. Kaplan, Eds. (Spec. Publ. no. 3, Geochemical Society, San Antonio, TX 1991), p. 27.
- We crushed and sieved natural perovskite crystals to obtain size fractions with mean radii of 12, 18, and 26 μm . Aliquots of CaTiO₃ powder were placed in perforated Pt crucibles that were suspended in a vertical muffle-tube furnace and exposed to pure CO₂ gas flow. Oxygen was liberated from the perovskite with BrF₅ and analyzed on the mass spectrometer. Diffusion coefficients were calculated on the assumption that diffusion was from an infinite volume of gas into spherical grains, with the use of formulations from W. Jost [*Diffusion in Solids, Liquids and Gases* (Academic Press, New York, 1960)]. The experimental procedure is detailed by B. Gautason [thesis, University of Alberta (1992)]. A copy of the complete data table is available on request.
- E. Dowty, *Am. Mineral.* **65**, 174 (1980).
- Oxygen diffusion rates in silicates under hydrothermal conditions are described by an equation of the same form but with different constants [S. M. Fortier and B. J. Giletti, *Science* **245**, 1481 (1989)].
- The values differ from those published previously (7). Here the model is applied to a closely packed mineral, and therefore we include data from low-porosity minerals such as sapphire (25.5%) and spinel (36.2%) to derive the constants.
- R. E. Cohen, *Geophys. Res. Lett.* **14**, 1053 (1987).
- Y. Fei, H.-K. Kwang, R. J. Hemley, J. Shu, in *Annual Report of the Director of the Geophysical Laboratory* (Carnegie Institution of Washington, Washington, DC, 1991), p. 107.
- R. M. Hazen and L. W. Finger, *Comparative Crystal Chemistry* (Wiley, New York, 1984).
- T. Yagi, H. K. Mao, P. M. Bell, *Phys. Chem. Miner.* **3**, 97 (1978); H. Horiuchi, E. Ito, D. J. Weidner, *Am. Mineral.* **72**, 357 (1987).
- S. R. Hart, *Geochim. Cosmochim. Acta* **45**, 279 (1981).
- O. L. Anderson, *Philos. Trans. R. Soc. London Ser. A* **306**, 21 (1982).
- Our conclusions are not critically sensitive to the calculation of Φ because of the anchoring effect of the isokinetic temperature (T_i). For any porosity profile, the oxygen diffusion rate at T_i (~ 1100 km depth) is the same. For instance, if one assumes that the ionic radius of oxygen in perovskite is 1.36 Å at 1 bar, then the calculated porosity will decrease from 23% to 17%. The calculated diffusion profile will cross the one in Fig. 4 at T_i , and calculated oxygen diffusion rates will not deviate by more than a factor of 5 from the values shown in Fig. 4.
- R. M. Dell and A. Hooper, in *Solid Electrolytes*, P. Hagenmuller and W. Van Gool, Eds. (Academic Press, New York, 1978), p. 291.
- B. Kapusta and M. Guillope, *Philos. Mag.* **58**, 809 (1988); G. D. Price, A. Wall, S. C. Parker, *Philos. Trans. R. Soc. London Ser. A* **328**, 391 (1988); A. Wall and G. D. Price, *Phys. Earth Planet. Inter.* **58**, 192 (1989); M. Matsui and G. D. Price, *Nature* **351**, 735 (1991); B. Kapusta and M. Guillope, *Phys. Earth Planet. Inter.* **75**, 205 (1993).
- The oxygen diffusion rates predicted for the base of the lower mantle are similar to those obtained for solid-oxide fuel cells with perovskite structure and the "1-2-3" superconductors at 1 atm and $T \leq 1000^\circ\text{C}$. The high diffusivities in these phases are facilitated by a high concentration of anion vacancy, forced by introduction of mixed valence cations on the A site, B site, or both. See, for example, H. Bakker, J. P. A. Westerveld, D. O. Welch, *Physica C* **153-155**, 848 (1988); S. Carter *et al.*, *Solid State Ionics* **53-56**, 597 (1992).
- Early work by D. C. Tozer suggested that ionic

- conductivity is not an important conductivity mechanism in the lower mantle. He calculated the temperature T_c where ionic conductivity equals electronic conductivity for an olivine-dominated mantle, as a function of pressure. He found that T_c is significantly higher than projected mantle temperatures [D. C. Tozer, *Phys. Chem. Earth* 3, 414 (1959)].
23. X. Li and R. Jeanloz, *Geophys. Res. Lett.* 14, 1075 (1987); J. Peyronneau and J. P. Poirier, *Nature* 342, 537 (1989); X. Li and R. Jeanloz, *J. Geophys. Res.* 95, 5067 (1990); *Nature* 350, 332 (1991); B. J. Wood and J. Nell, *ibid.* 351, 309 (1991); X. Li *et al.*, *J. Geophys. Res.* 98, 501 (1993).
24. N. F. Mott and R. W. Gurney, *Electronic Processes in Ionic Crystals*, (Dover, New York, 1964).
25. J. Ducruix, V. Courtilot, J. L. Mouel, *Geophys. J. R. Astron. Soc.* 61, 73 (1980).
26. References for data in Table 1 are as follows: for nepheline and diopside, C. Connolly and K. Muehlenbachs, *Geochim. Cosmochim. Acta* 52, 1585 (1988); melilite, T. Hayashi and K. Muehlenbachs, *ibid.* 50, 585 (1986); anorthite, S. C. El-

- phick, C. M. Graham, P. E. Dennis, *Contrib. Mineral. Petrol.* 100, 490 (1988); forsterite, K. Ando, H. Kurokawa, Y. Oishi, *J. Am. Ceram. Soc.* 64, C30 (1981) and O. Jaoul, B. Houlier, F. Abel, *J. Geophys. Res.* 88, 613 (1983); quartz, P. F. Dennis, in *Progress in Experimental Petrology*, C. M. B. Henderson, Ed. (Cambridge Univ. Press, Cambridge, 1984), p. 260; SiO₂ glass, H. A. Schaeffer and K. Muehlenbachs, *J. Mater. Sci.* 13, 1146 (1978); Mg-spinel, K. Ando, Y. Oishi, *J. Chem. Phys.* 61, 625 (1974); Mg-spinel, K. P. R. Reddy and A. R. Cooper, *J. Am. Ceram. Soc.* 64, 368 (1981); MgO and α -Fe₂O₃, K. P. R. Reddy and A. R. Cooper, *ibid.* 66, 664 (1983); and sapphire, K. P. R. Reddy and A. R. Cooper, *ibid.* 65, 634 (1982).
27. We thank T. Chacko, R. W. Luth, J. Farquhar, J. Staveley, and two anonymous reviewers for constructive comments and O. Levner for assistance with analyses. Supported by the Natural Sciences and Engineering Research Council of Canada.

29 September 1992; accepted 22 January 1993

The Relation Between Biological Activity of the Rain Forest and Mineral Composition of Soils

Y. Lucas,* F. J. Luizão, A. Chauvel, J. Rouiller, D. Nahon

In most soils of the humid tropics, kaolinitic topsoil horizons overlie more gibbsitic horizons. This arrangement cannot be produced simply by leaching. Quantitative measurement of the turnover of chemical elements in the litterfall in an Amazonian ecosystem indicates that the forest cycles a significant amount of elements, particularly silicon. As a result, fluids that percolate through topsoil horizons already contain dissolved silicon. This effect keeps silicon from being leached down and may account for the stability of kaolinite in the soil upper horizons. The soil mineral composition is thus maintained by biological activity.

Tropical acid soils are composed of residual primary minerals, mainly quartz grains (SiO₂), and newly generated secondary minerals, mainly kaolinite [Al₂Si₂O₅(OH)₄] and smaller quantities of gibbsite [Al(OH)₃], hematite (Fe₂O₃), and goethite (FeOOH). In most of the well-drained, nonspodic acid soils under tropical humid climates, kaolinite is the prevailing secondary mineral in the topsoil horizons. The observed gibbsitic horizons appear to be situated beneath more kaolinitic horizons as gibbsitic saprolite, nodular or bauxitic horizons, or gibbsite accumulations in a kaolinitic matrix (1–3). From a chemical standpoint, these soils are more siliceous on the top horizons and more aluminous underneath. This structure of the soil profile is observed for old soils, such as Amazonian bauxites, as well as for young soils.

Y. Lucas, Núcleo de Pesquisa da Geoquímica da Litosfera and Institut Français de Recherche Scientifique pour le Développement en Coopération, Université de São Paulo, CP 9638, 01065 São Paulo, Brazil.

F. J. Luizão and A. Chauvel, Instituto Nacional de Pesquisas da Amazônia, Laboratório de Ecologia, CP 478, 69060 Manaus, Brazil.

J. Rouiller, Centre de Pédologie Biologique, 54500 Vandœuvre-les-Nancy, France.

D. Nahon, Université Saint-Jérôme, Géosciences de l'Environnement, 13397 Marseille Cedex 13, France.

*To whom correspondence should be addressed.

This observed vertical succession is just the opposite of that predicted by most geochemical soil formation models (4–7). These models take a low-Si and -Al rain-water input on topsoil into consideration. As the water percolates, the solution-mineral reactions lead to a progressive increase of the Si and Al concentration in the soil solution. The models predict a vertical succession of horizons, with more aluminous gibbsitic horizons in the topsoil above the more siliceous kaolinitic horizons. The discrepancy between the models and the observed soil horizons has long been ignored for two reasons. There has been a lack of field studies on humid tropical soil geochemistry, and the top horizons of tropical soils have been frequently interpreted as allocthonous, that is, the kaolinitic material was deposited after the lower soil layers had formed. Numerous studies in the last 20 years, however, have pointed out that such allocthony is more restricted than had been thought. Most of the tropical soils have formed in situ (8, 9), with a possible input of foreign material by dust deposition (10). Various other explanations of the siliceous topsoil production have already been proposed: uplift of deep material by termites or ants (11); rapid percolation of the rainwater

through the topsoil so that water-mineral interaction does not reach equilibrium (12); or decreased water activity in the topsoil during dry seasons, displacing the kaolinite-gibbsite equilibrium (13). These hypotheses rarely apply to humid tropical soils, however. Termite or ant activity is normally restricted to the upper horizons of soil where the dry season is short. Water generally percolates slowly through soils as capillary water (14). During exceptionally dry periods, soil suction can reach 15 bars, which is the usually accepted limit for plant wilting. Under these conditions, maximum water activity changes would be from 1 to 0.989, which correspond to a quite small (+0.55%) shift of the dissolved SiO₂ concentration at the gibbsite-kaolinite equilibrium.

To investigate the source of this permanent Si stock above more aluminous horizons, we studied the role of the rain forest itself on the geochemical cycling of the elements that act on the mineral-solution reactions, paying special attention to Si. The potential effect of plants on element cycles in soils has long been apparent (15, 16), but only limited data are available for Si or Al (17, 18), especially in the tropics. Here we evaluate the element turnover in the forest annual litterfall and the total Si content of the forest, as well as the potential influence of elemental cycling in the forest on soil mineral composition.

Our study site was 80 km north of Manaus, Brazil (02°34'S, 60°07'W). The climate is equatorial; average annual rainfall is 2100 mm and the dry season lasts 3 months. The landscape is a plateau covered by a typical Amazonian rain forest (19). Soils (20) consist of a 3- to 8-m-thick kaolinitic clay overlying a more gibbsitic 3-m-thick nodular horizon (Fig. 1). The mean ratio of kaolinite to gibbsite decreases from 14 in the upper clay to 3 in the nodular horizon. These soils were formed by a progressive desilicification of the sandy-clay parent sediment. The progressive ver-

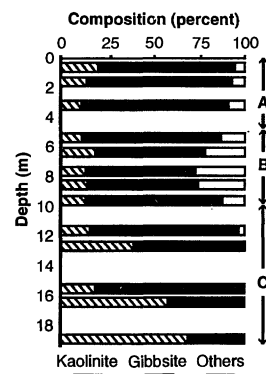


Fig. 1. Mineralogical composition of the soils. (A) Upper clay horizon, (B) nodular horizon, and (C) saprolite.